Journal Pre-proof

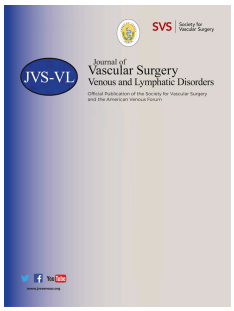

Magnetic Resonance Lymphangiography: Establishing Normal.

Mike Mills, Greta Brezgyte, Bernard Ho, Julian Pearce, Kristiana Gordon, Peter S. Mortimer, Pia Ostergaard, Franklyn A. Howe

PII: S2213-333X(24)00161-6

DOI: https://doi.org/10.1016/j.jvsv.2024.101870

Reference: JVSV 101870

To appear in: *Journal of Vascular Surgery: Venous and Lymphatic Disorders*

Received Date: 21 December 2023

Revised Date: 4 March 2024

Accepted Date: 6 March 2024

Please cite this article as: M. Mills, G. Brezgyte, B. Ho, J. Pearce, K. Gordon, P.S Mortimer, P. Ostergaard, F.A Howe, Magnetic Resonance Lymphangiography: Establishing Normal., *Journal of Vascular Surgery: Venous and Lymphatic Disorders* (2024), doi: https://doi.org/10.1016/j.jvsv.2024.101870.

Magnetic Resonance Lymphangiography: Establishing Normal.

Short Title: MRL of controls

Authors

Mike Mills[1 *], Greta Brezgyte[2], Bernard Ho[3], Julian Pearce[3], Kristiana Gordon[2,3], Peter S Mortimer[2,3], Pia Ostergaard[2], Franklyn A Howe[1]

Affiliations

1 - Neurosciences and Cell Biology Research Institute, St George's University of London, London, UK
2 - Cardiovascular & Genomics Research Institute, St George's University of London, London, UK
3 - Dermatology and Lymphovascular Medicine, St George's University Hospitals NHS Foundation Trust, London, UK
* - Corresponding author contact address: Cranmer Terrace, Tooting, London SW17 0RE, UK; e-mail: mmills@sgul.ac.uk

Conflict of Interest Statement

The authors have no competing interests.

Article Highlights

Type of Research: Single centre prospective observational study.

Key Findings: Lymphatic vessels following the anteromedial and anterolateral pathways were observed in most healthy limbs imaged (30/31). The vessels were superficial and linear (average tortuosity =1.09 ± 0.03 in the 27 vessels interrogated). Drainage of the contrast agent was slow, with signal often rising throughout the course of imaging.

Take home Message: Depiction of normal lymphatic vessels in non-lymphoedematous limbs can be observed following Gadolinium-based contrast injections in the forefoot, and metrics related to lymph drainage rate, lymphatic vessel size and tortuosity are measurable.

Table of Contents Summary

MR Lymphangiography (MRL) reliably depicts the lymphatic vessels of healthy individuals' lower limbs, which follow the expected anatomical pathways after contrast injection to the forefoot. Definition of normal anatomy and function is therefore possible with MRL, further supporting its use as a tool to study the lymphatic system.

Abstract

Background: Despite an increased interest in visualising the lymphatic vessels (lymphatics) with Magnetic Resonance Lymphangiography (MRL), there remains little literature describing their appearance in non-lymphoedematous individuals. To determine lymphatic abnormalities, an understanding of how healthy lymphatics appear and behave needs to be established. In this study, MRL of individuals without a history of lymphatic disease was therefore performed.

Methods: A total of 25 individuals (15 female) underwent MRL of their lower limbs using a 3.0T Philips MRI scanner. The first 9 cases were recruited to establish the concentration of Gadolinium-based contrast agent (GBCA) to administer, with the remainder imaged pre- and post-inter-digital forefoot GBCA injections at the optimised dose. Outcomes including lymphatic vessel diameter, tortuosity and the frequency of drainage via particular drainage routes were recorded.

Results: Healthy lymphatics following the anteromedial pathway were routinely observed in post-contrast T_1 weighted images (average tortuosity = 1.09 ±0.03), with an average of 2.16 ± 0.93 lymphatic vessels, of diameter 2.47 ± 0.50 mm, crossing the anterior ankle. In six limbs, vessels following the anterolateral pathways were observed. No vessels traversing the posterior of the legs were seen. In a subset of ten vessels lymphatic signal, measured at the ankle, peaked 29:50 ± 09:29 mm:ss after GBCA administration. No lymphatic vessels were observed in T_2 weighted images.

Conclusions: Contrast-enhanced MRL reliably depicts the lymphatics in the legs of healthy controls. Following inter-digital contrast injection, anteromedial drainage appears dominant. Quantitative measures related to lymphatic vessel size, tortuosity and drainage rate are readily obtainable, and could be beneficial for detecting even subtle lymphatic impairment.

Keywords

Magnetic Resonance Imaging; Lymphography; Lymphatic Vessels; Lower Extremity

Funding Statement

This work was supported by a joint grant from the Medical Research Council and the British Heart Foundation (Ref: MR/P011543/1 and RG/17/7/33217), with no direct involvement of the sponsors.

Introduction

The lymphatic system is arguably the most neglected bodily system and so its contribution to human health and disease is poorly understood. Lymphoedema, the chronic swelling of tissues due to a failure of the lymphatic system, is estimated to affect between 140-250 million people worldwide, but remains insufficiently characterised (1). Genes and molecular proteins specific to the lymphatic system have been discovered only relatively recently. This has enabled a greater understanding of lymphatic development and the active role of lymphatics in cellular and physiological processes, but knowledge of human lymphatic disease remains limited by a lack of reliable investigatory techniques. Blood vessels such as veins are visible to the naked eye and can be studied using non-invasive duplex ultrasound examination. Lymphatic vessels are not easily seen and cannot be reliably imaged without the aid of an exogenous contrast medium.

Hudack and McMaster injected their skin with a blue dye in 1933, observing how quickly the dye flowed through their dermal lymphatics, sparking an interest in imaging the lymphatics (2). Following this, X-ray imaging after the administration of a suitable contrast agent to cannulated lymphatics facilitated visualisation of larger collecting vessels. The first human lymphangiograms were produced by John Kinmonth in 1952 and demonstrated lymphatics from foot to groin (3). This resulted in a better understanding of many forms of lymphoedema, especially primary lymphoedema. While direct contrast X-ray lymphography gives highly detailed images of collecting lymphatics in the lower limbs, the procedure is invasive and not without risk (e.g., lipiodol induced embolism of the vessel) so is now rarely used (4). Indocyanine Green Lymphography (ICG-L) provides *in-vivo* real-time imaging of lymphatic vessels but is limited to imaging only the most superficial vessels. Lymphoscintigraphy (LS) is the current clinical investigation for diagnosis but functional rather than anatomical detail is provided. Magnetic Resonance Lymphangiography (MRL) can provide detail of the lymphatics in greater detail than LS, without the associated ionising radiation, and is not limited by penetrance; a drawback of ICG-L (5).

To determine what is abnormal, one must know what is normal. Despite the improved imaging detail, MRL has not facilitated the identification of lymphatic structures universally in those publications imaging non-affected limbs, so what constitutes a normal MRL is still unclear (6). In this report we share our experience of identifying the lymphatics with MRL in healthy subjects with normal lower limbs. Since this study is on healthy individuals it provides a normal baseline for MRL, unlike studies of the contralateral limb of unilateral lymphoedema patients, a potentially problematic comparison group given that reports of lymphatic dysfunction in these clinically asymptomatic limbs have been reported (7,8). Our aim was therefore to determine if MRL is a robust and tolerable method of visualising lymphatic vessels and nodes, and able to establish the anatomy and function in individuals unaffected by lymphoedema.

Methods

Participants

The healthy individuals included in this study were recruited as part of an ongoing programme of research to improve understanding of the causal mechanisms and implications of primary lymphoedema. This programme includes investigations of the limb lymphatics of primary lymphoedema patients and healthy individuals with MRL (approved by the London – Camden & Kings Cross- Research Ethics Committee, 20/LO/0237), with healthy participants (predominantly staff, students, and unaffected spouses of lymphoedema patients) recruited and imaged to both improve understanding of the anatomy and physiology of healthy limb lymphatics and to provide an

approximately age and sex matched comparison group for the lymphoedema cohort. This article focusses on improving the understanding of healthy lower limb lymphatics and so exclusively reports on participants without a lymphoedema diagnosis. Participant demographics are summarised in Table 1.

Injection Protocol

All participants received a diluted mixture of 0.5M Gadolinium-based contrast agent, GBCA, (Dotarem®, Guerbet) saline and 1% lidocaine anaesthetic in 1mL volumes per injection. Injections were performed intradermally in each of the four interdigital spaces of the foot, as is routine in the MRL literature (6,9), by hand and at a slow rate (each injection typically lasting between 15 and 60 seconds) by Dermatologists.

Dose Optimisation

Nine participants (3 male and 6 female) were initially enrolled to investigate the effect of the concentration of GBCA (either 0.02mL/mL, 0.1mL/mL or 0.45mL/mL of the volume administered) on the visibility of lymphatic vessels, with the concentration considered to deliver the clearest and most consistent lymphatic enhancement being employed thereafter. For some participants, a different GBCA concentration was administered to each limb in order to facilitate a direct contralateral comparison (Figure 1). This optimisation was performed dynamically, such that if a GBCA dose was unable to depict lymphatic vessels after multiple attempts it was removed from consideration.

Imaging Protocol

All participants were imaged feet-first supine using a 3.0T system (Dual TX Achieva, Philips Medical Systems, Netherlands) with a 16-element torso receiver coil positioned around the leg (ankle to knee). Lower limbs were imaged pre-contrast administration with a heavily T_2 weighted 3D turbo-spin echo sequence, and pre- and post-contrast with moderately T_1 weighted 3D spoilt gradient echo imaging (See Table 2 for details). The T_1 weighted sequence was repeated in a dynamic manner for approximately 30 minutes immediately following bilateral contrast injection to the feet. The imaged volume generally included the region from mid-foot to just below the knee. A subset of participants underwent T_1 weighted Dixon imaging from knee-mid thigh. A Dixon imaging approach was chosen for this anatomical region as more robust fat suppression was required (10). These images in the thigh were typically collected ~30-40 minutes after the commencement of contrast-enhanced imaging.

Data Collection, Outcome Measures and Analysis

Anatomy

Lymphatic vessels were identified predominantly by their characteristic beaded and tortuous appearance, and were distinguished from veins which were anticipated to be straighter and of uniform and larger calibre (Figure 2) (11–14). Based on the path taken in the limb, lymphatic vessels were classified as belonging to one of four groups: anteromedial, posteromedial, anterolateral and posterolateral, as described by Shinaoka *et al.* (15). Identification of vessels was first attempted using the heavily T_2 weighted images, before moving on to the dynamic T_1 datasets. For the latter, maximum intensity projection (MIP) images were produced in which the first post-contrast image was subtracted from all subsequent dynamics, as described previously (16). The presence of any lymph nodes in the popliteal fossa (popliteal nodes) was also recorded when this region was imaged.

The presence of features such as: dermal rerouting, markedly tortuous or transverse lymphatic vessels as seen in T_1 weighted images, and hyperintense, fluid-rich, regions of T_2 weighted datasets, were considered abnormal findings and recorded.

Estimates of the **number of lymphatic vessels** crossing the anterior ankle, and their **diameter** (taken as the full width at half maximum extent), were also recorded. **Lymphatic vessel tortuosity** for a single vessel in each leg was estimated as:

$$Tortuosity\ Index = \frac{Distance\ between\ vessel\ segment\ endpoints}{Vessel\ length}$$

after the lymphatic vessel was manually segmented and its centreline extracted using the Vascular Modelling Tool Kit module implemented in 3D Slicer (17–19). The chosen vessel had to have been characterised as belonging to the anteromedial pathway and have a minimum length of 200mm.

Lymphatic Transport

The rapidity of GBCA drainage, a proxy for lymphatic function, was interrogated in each leg of a subset of 5 individuals (3 male and 2 female controls; average age = 34.1 ± 9.9 years). Image signal was measured in 3x3x3 voxel regions centred over a lymphatic vessel just superior to the ankle (Figure 2) and the time from contrast injection to peak signal (T_{peak}) estimated. The lymphatic signal was normalised to the adjacent muscle to account for signal drift across the timeseries. The same procedure was also carried out in the great saphenous vein just above the ankle and compared to the lymphatics via an independent samples t-test. All statistical analyses were conducted with SPSS (IBM, SPSS Statistics 29.0, Chicago, IL), and $p < 0.05$ considered the threshold for statistical significance.

Results

MRL was successful in all participants without complications. The slight discomfort of injections was well tolerated due to the use of a local anaesthetic.

Injection dose optimisation

Inspection of the images from the 18 limbs studied (two injected with 0.02mL/mL GBCA containing solutions, 6 with 0.1mL/mL, 10 with 0.45mL/mL) demonstrated lymphatic structures in all of those administered 0.45mL/mL GBCA formulations, compared to only half at 0.1mL/mL and none at 0.02mL/mL concentrations respectively. In the limbs receiving the highest GBCA concentration, both veins and lymphatic vessels appear brighter (Figure 1). The 0.45mL/mL protocol was adopted as the dose regime for the subsequent participants, therefore all following results refer to those limbs administered with this GBCA concentration, and exclude those 9 individuals imaged as part of the contrast optimisation process.

Main Imaging Study

Leg

After contrast optimisation, 16 further individuals were recruited (7 male, 9 female) creating 32 leg examinations. A single limb was excluded from our analysis, leaving 31 to be analysed. This exclusion was due to a technical fault, presumed to originate from poor contact between the coil connector and the scanner, which led to severe signal loss affecting a single limb. In all but a single limb lymphatic vessels could be visualised during the dynamic T_1 imaging, while in none of the 31 healthy limb datasets could lymphatics be observed on T_2 weighted imaging.

The **number of vessels** noted crossing the anterior ankle ranged from 0 - 4 (mean ± standard deviation = 2.16 ± 0.93, modal count = 3) (Figure 3A-C). The predominant drainage pathway observed was the anteromedial (29/31), with the anterolateral the only other pathway observed (6/31) (Figure 3C). Supplementary Table 1 details the number of enhancing lymphatic vessels and pathways for each participant. Mean **vessel diameters** were measured at 2.47 ± 0.50 mm (range =

1.56 - 3.75 mm), and all detected lymphatic vessels resided superficially in the leg (<2 cm from the closest skin boundary).

No transverse lymphatic vessels, regions of dermal rerouting or any potential signatures of lymphatic dysfunction were noted, and no lymphatic vessels appeared abnormally tortuous. Mean **tortuosity** ± standard deviation was measured at 1.09 ± 0.03 in 27 vessels anteromedial, with vessels in two limbs excluded from analysis due to lengths below 200mm (Figure 4, Supplementary videos 1 and 2 demonstrate 360° coronal projections of the same vessel segment).

Thigh

Of those participants where imaging above the knee was performed (26 limbs), in just 6 could lymphatics vessels be confidently detected using the post-contrast T_1 weighted images (data not shown). In all cases these vessels were observed progressing superficially up the medial knee and thigh towards the inguinal region. No popliteal nor any other lymph nodes were observed in any participants.

Fluid Accumulation

A single individual did not undergo this portion of imaging due to timing constraints. In the remaining 29 available limb datasets, the majority of participants did not demonstrate substantial areas of high signal, indicative of static fluid, beyond that noted within the joints. A single individual's limbs were noteworthy for having demonstrated hyperintense regions throughout the limb, with bilateral regions of particularly high signal in the medial mid-leg (Figure 5).

Lymphatic Transport

Significantly quicker peaking of the signal was observed in the veins compared to lymphatics (mean ± standard deviation T_{peak} = 15:50 ± 03:06 and 29:50 ± 09:29 respectively, $p < 0.05$) (Figure 6). Additionally, in 4/10 control limbs, the lymphatic signal peaked in the final imaging phase, compared to only a single incidence of this recorded in the veins. Peak venous signal, normalised to the muscle, was also higher compared to the lymphatics (mean ± standard deviation = 1.41 ± 0.46 and 2.71 ± 0.62 in lymphatic vessels and veins respectively, $p < 0.05$). Average normalised uptake curves for veins and lymphatic vessels are displayed in supplementary Figure S1, where for each vessel the signal was scaled to take on value between 0-1 before averaging across the 10 vessels interrogated.

Discussion

Summary

Various lymphatic imaging techniques, including indocyanine green lymphography (ICG-L) and lymphoscintigraphy (LS), have been successfully deployed to image the lymphatics following injections of an external agent into the feet. These techniques however are limited to producing 2D images of the lymphatics with poor spatial resolution in the case of LS, and poor penetrance for ICG-L. MRL appears well placed to overcome these shortcomings, however visualising healthy lymphatics with MRL has been reported as problematic (6). In this study, we investigated whether MRL is capable of depicting, and estimating markers of function within, healthy leg lymphatics at 3.0T. We aimed to provide information related to normal lymphatic anatomy and physiology, and demonstrate features which may be beneficial in the detection of lymphatic abnormalities and arriving at a lymphoedema diagnoses. Enhancement of lymphatic vessels belonging to the anteromedial or anterolateral drainage routes were observed in all but a single limb following inter-digital injections of a Gadolinium-based contrast agent (GBCA) in the forefoot, confirming that MRL is indeed a robust tool for depicting lymphatic vessels in healthy legs. Further, measurements related to lymphatic

shape and ability to transport the administered GBCA were demonstrated within the leg. Depiction of lymphatics in the thigh was not commonly observed (6/26 thighs), a result we believe is at least in part due to the long delay (a minimum of 30 minutes) between contrast injection and imaging this region.

Contrast Optimisation

Depiction of normal lymphatic anatomy and estimates of their function are key in improving the utility of MRL for detecting abnormalities, yet a failure to visualise lymphatic vessels in healthy subjects has been reported in multiple studies (20–22). In addition, contrast enhancement of veins can lead to ambiguity in identification of lymphatic vessels, and there are concerns about the safety of GBCA. We therefore explored the effect of GBCA dose on the visibility of lymphatic vessels in a subset of our participants. Two attempts administering 0.02mL/mL, which had previously been administered in the arms of individuals with a breast cancer-related lymphoedema (BCRL) and controls to successfully reduce the effect of venous enhancement (23), elicited no clear lymphatic enhancement in this study, and no further attempts with this protocol were attempted. At a concentration of 0.1mL/mL the venous signal was reduced compared to 0.45mL/mL, however there was also a major loss of lymphatic signal that was considered too costly to warrant adoption of this reduced GBCA protocol. We did not try to administer GBCA undiluted (i.e. administered with local anaesthetic, but without further dilution) given that in all limbs administered with 0.45mL/mL the lymphatics could be observed and so increasing the total GBCA volume administered was deemed unnecessary. However, this does prevent us from commenting on whether at 0.45mL/mL the venous signal is reduced relative to the lymphatics as compared to when GBCA is given undiluted. Studies exploring optimal contrast injection protocols (contrast agent formulation, dose, local massage, etc.) balancing the trade-off between safety, lymphatic, and venous signal are still required: though the risk of an adverse event is small, total GBCA doses administered should always be as low as is practicable.

Normal vs. Abnormal Lymphatics

Based on the work of Shinaoka *et al.* (15), who imaged non-lymphoedematous cadaver's lower limbs with ICG-L and CT, we anticipated forefoot injections to elicit contrast drainage via vessels belonging predominantly to the anteromedial pathway. We confirmed this, with enhancing anteromedial lymphatics seen in the majority of limbs (29/31 limbs). In approximately a fifth of cases, including a single limb not demonstrating anteromedial lymphatic enhancement, anterolateral vessels were observed. The presence of anterolateral lymphatic enhancement should therefore not necessarily be considered pathological collateralisation following forefoot contrast injections. Again, in agreement with the aforementioned cadaver study, we observed that all enhancing vessels remained superficial and hence anticipated the finding that no enhancement of popliteal lymphatic nodes is observed. We, and others, have noted collateral posterior lymphatic drainage following inter-digital contrast administration in cases of lymphoedema however (Figure 7), with Soga *et al.*, also reporting popliteal node enhancement when imaging lymphoedema patient's lower limbs at 1.5T (24).

The results of our investigation of lymphatic tortuosity confirm that, while the collector vessels of lymphoedema patients are often reported as being abnormally tortuous, the lymphatics of healthy individuals appear relatively linear by comparison (25–27). We have built upon the descriptive results of prior studies by computing absolute tortuosity in lymphatic vessel segments, a value which is simple to compute and may be used to better stratify normal and abnormal lymphatic vessels. Further highlighting the readily quantifiable nature of MRL, we recorded the elapsed time between the commencement of GBCA injection and signal peak in regions of anteromedial lymphatic vessels and adjacent great saphenous vein. The signal in the lymphatic vessels peaked significantly later than

the veins, as has been previously reported (23), and showed lower variability in T_{peak}. This clustering may be somewhat artificial given that in 4/10 vessels the signal was still rising at the cessation of imaging. This will also likely have reduced the true difference in T_{peak} between vessel types, further highlighting the potential for this measurement to be used to separate lymphatic and venous structures. Additionally, this assessment has been used to compare lymphatic contrast uptake rates in cases of Lymphoedema Distichiasis Syndrome (LDS) compared to healthy controls, in which lymphatic signal peaked significantly more rapidly in LDS patients (28).

The healthy nature of our cohort also meant that in all cases T_2 weighted imaging highlighted no lymphatic vessels and few areas of fluid accumulation outside of the joints, both of which have been reported in studies imaging lymphoedema patients (29,30). A single individual demonstrated particularly extensive intense regions on T_2 imaging compared to the other controls, but substantially less than can be observed in many lymphoedema patients (Figure 4). It was remarked by the clinician performing the GBCA injection (P.S.M.) during the pre-imaging examination that they believed this individual showed clinical signs indicative of lipoedema, which may explain the difference in image appearance for this case. This individual demonstrated normal appearing lymphatic vessels, however, and removing their data from the analysis has very little effect, with the average vessel count at the ankle = 2.21 ± 0.94 and their diameter = 2.48 ± 0.50 mm (compared to 2.16 ± 0.93 and 2.47 ± 0.50 mm prior to the exclusion).

Strengths and Weaknesses of MRL

As mentioned prior, MRL has some key advantages over alternative imaging techniques: improved spatial resolution and non-ionising nature compared to LS, and an ability to visualise lymphatic vessels beyond the most superficial compared to ICG-L, as well as being able to depict both the lymphatics and soft-tissues in a 3D manner. There exist some weaknesses of the technique which need addressing however. Foremost amongst these is that intra-dermal GBCA injection causes both lymphatic and venous enhancement, which can lead to difficulty in assigning enhancing vessels as being of a lymphatic or venous origin. The generally smaller and discontinuous appearance of the lymphatics aids in their identification, and we have also found the use of subtraction images further assists with differentiation (16). The use of prospective measures to combat venous enhancement may be of particular benefit in lymphoedema patients where dilated lymphatics have been observed (31). Administration of an ultra-small superparamagnetic iron oxide (USPIO) agent either into the bloodstream, reducing the blood's T_2 value and signal, or as an interstitial agent which is preferentially trafficked into the lymphatics, shows great potential (32,33). Despite these promising results, we have yet to adopt this agent for use in our own studies as, at the time of writing, the agent remains unlicensed for use as an MR contrast agent in the United Kingdom. Our observation of a more rapid wash-in and wash-out of contrast agent in the great saphenous vein compared with proximal lymphatic vessels may offer an additional avenue for improving identification of venous and lymphatic structures based on their uptake characteristics. Whether this difference holds in lymphoedema patients is yet to be established. This difference also helps to explain the benefit of subtracting the initial post-contrast image from all subsequent images regarding lymphatic visibility: any venous enhancement beyond this initial imaging phase is likely to be small compared to the change in lymphatic signal over time.

At present MRL has only been used to demonstrate the larger lymphatic vessels with T_1 weighted imaging resolutions typically of the order of 1mm isotropic (9). To image smaller vessels and the pre-collector vessels proximal to contrast injection sites, further optimisation of the imaging and contrast injection protocol may be required. It has been noted for example that with higher concentrations of

GBCA injection a loss of signal at the injection site can occur (23). Imaging at higher field strengths may therefore be required for these vessels given the resultant boost to image signal.

MRL is also limited by all contraindications which prevent participants from undergoing any MR-based examination (implanted medical device, claustrophobia etc.). People with a previous history of allergies to contrast agents or other medications may also be prevented from proceeding with a contrast-enhanced study, however many studies have demonstrated the utility of non-contrast in assessing lymphatic disease (8,27,34). In any case, the administration of GBCA intra-dermally is considered off-label use and so care must be taken by the administering clinician to thoroughly consider the risks and benefits of GBCA injection. As with many previous studies, we report no adverse events associated with this type of contrast injection however (35,36).

Study Weaknesses and Future Work

We acknowledge that this study is limited by several factors. We recruited healthy controls from a local population which may not be indicative of the wider population and did not image children. Secondly, we performed quantitative assessment of lymphatic uptake rates and vessel tortuosity on only a single vessel in the limbs studied. Future studies would benefit both from exploring all viable vessels and exploring the repeatability of these measurements. The choice of metrics may also not be the most sensitive for detecting pathological changes, for example curvature-based estimates may prove a better probe of changes in lymphatic vessel morphology than tortuosity, as was recently shown in a study exploring blood vessel changes associated with coronary artery disease (37). This study is also limited by the lack of patient data. We are currently in the process of collecting patient MR datasets, for which this work relating to healthy controls will be of great value as a comparison group without signs of lymphatic disease.

Lymphatic dysfunction has been associated with fat deposition in addition to increased fluid, and MRI has been used to show this within individuals with a breast cancer-related lymphoedema diagnosis, and in which the non-oedematous limb was used as an internal comparison to the affected side (38). In the same paper, reduced T_2 values were seen to correlate with increased fat deposition providing further evidence of a disrupted tissue environment in cases of lymphoedema and how MRI can be used to assess this. Though we did not attempt to quantify fat volume or fraction in this study, fat-sensitive Dixon imaging, both within the leg and thigh, is now performed in both our unaffected and lymphoedematous research subjects, and we will explore this tissue compartment in future studies.

We did not explore the effect of alternative injection sites in relation to the depiction of deep lymphatic pathways. The ability to demonstrate these deeper lymphatics is considered a particular differential between MRL and ICG-L. The adoption of contrast injection to the lateral malleolus, as is performed in some ICG-L studies (39), should be explored in the future to explore the additional benefits of imaging the lymphatics with MRI. This should be performed first in healthy individuals given that posterior lymphatic enhancement from forefoot injections has been observed in some lymphoedema patients with MRL(24). Additionally, the effect of imaging the thigh sooner after contrast injection should be explored and whether this improves the visibility of lymphatic vessels in the region, or if higher GBCA concentrations or injected volumes are required.

Conclusion

Before MRL becomes a clinical and research mainstay for investigating lymphatic dysfunction, it must

be shown to be well tolerated by, and provide robust demonstration of the lymphatic anatomy within, healthy subjects. This study illustrates that with an appropriate contrast injection and imaging protocol, lymphatic vessels can be routinely identified in the limbs of healthy controls and simple quantitative values associated with lymphatic anatomy and drainage can be obtained. These findings were established in a broad age range of both male and female controls, which we believe to be of particular significance given that the manifestation of lymphoedema (primary or secondary) affects both men and women at any age.

Confirming the appearance and behaviour of healthy lymphatics on MRI is a valuable step toward establishing a comparison group for cases of lymphatic dysfunction. Moreover, it shows that the examination is well tolerated, and hence amenable to deployment in both the diagnosis of lymphatic disease and tracking the course of disease. The quantifiable nature of MRI (e.g. estimation of tissue compartment volumes, vessel sizes and rate of contrast uptake) position it well as an appropriate method for assessing treatment response. Further research of both healthy controls and patients is needed to identify suitable biomarkers, and to develop physiological models of GBCA movement, as has been achieved with contrast-enhanced MRI in oncology.

References

1. Földi M, Földi E. Földi's Textbook of Lymphology for Physicians and Lymphoedmema Therapists. 3rd ed. München: Urban & Fischer; 2012.

2. Hudack SS, McMaster PD. The lymphatic participation in human cutaneous phenomena: A study of the minute lymphatics of the living skin. Journal of Experimental Medicine. 1933;57(5):751–72.

3. KINMONTH JB. Lymphangiography in man; a method of outlining lymphatic trunks at operation. Clin Sci. 1952 Feb;11(1):13–20.

4. Lee B boong, Rockson SG. Lymphedema: A Concise Compendium of Theory and Practice. Second Edi. Lee BB, Rockson SG, Bergan J, editors. Cham: Springer International Publishing; 2018.

5. Liu NF, Lu Q, Liu PA, Wu XF, Wang BS. Comparison of radionuclide lymphoscintigraphy and dynamic magnetic resonance lymphangiography for investigating extremity lymphoedema. British Journal of Surgery. 2010 Mar;97(3):359–65.

6. Miseré RML, Wolfs JAGN, Lobbes MBI, van der Hulst RRWJ, Qiu SS. A systematic review of magnetic resonance lymphography for the evaluation of peripheral lymphedema. J Vasc Surg Venous Lymphat Disord. 2020;8(5):882-892.e2.

7. Burnand KM, Glass DM, Mortimer PS, Peters AM. Lymphatic dysfunction in the apparently clinically normal contralateral limbs of patients with unilateral lower limb swelling. Clin Nucl Med. 2012;37(1):9–13.

8. Franconeri A, Ballati F, Panzuto F, Raciti MV, Smedile A, Maggi A, et al. A proposal for a semiquantitative scoring system for lymphedema using Non-contrast Magnetic Resonance Lymphography (NMRL): Reproducibility among readers and correlation with clinical grading. Magn Reson Imaging. 2020;68(February):158–66.

9. Mills M, van Zanten M, Borri M, Mortimer PS, Gordon K, Ostergaard P, et al. Systematic Review of Magnetic Resonance Lymphangiography From a Technical Perspective. Journal of Magnetic Resonance Imaging. 2021;53(6):1766–90.

10. Del Grande F, Santini F, Herzka DA, Aro MR, Dean CW, Gold GE, et al. Fat Suppression Techniques for 3T MRI of The Musculoskeletal System. Physiol Behav. 2014;176(10):139–48.

11. Salehi BP, Sibley RC, Friedman R, Kim G, Singhal D, Loening AM, et al. MRI of Lymphedema. Journal of Magnetic Resonance Imaging. 2023;57(4):977–91.

12. Gennaro P, Borghini A, Chisci G, Mazzei FG, Weber E, Tedone Clemente E, et al. Could MRI visualize the invisible? An Italian single center study comparing magnetic resonance lymphography (MRL), super microsurgery and histology in the identification of lymphatic vessels. Eur Rev Med Pharmacol Sci. 2017;21(4):687–94.

13. Lohrmann C, Foeldi E, Langer M. Indirect magnetic resonance lymphangiography in patients with lymphedema preliminary results in humans. Eur J Radiol. 2006 Sep;59(3):401–6.

14. Notohamiprodjo M, Baumeister RGH, Jakobs TF, Bauner KU, Boehm HF, Horng A, et al. MR-lymphangiography at 3.0T - A feasibility study. Eur Radiol. 2009;19(11):2771–8.

15. Shinaoka A, Koshimune S, Suami H, Yamada K, Kumagishi K, Boyages J, et al. Lower-limb lymphatic drainage pathways and lymph nodes: A CT lymphangiography cadaver study. Radiology. 2020;294(1):223–9.

16. Mills M, Gordon K, Ratnam L, Zanten MVAN, Mortimer PS, Ostergaard PIA, et al. Image registration and subtraction in dynamic magnetic resonance lymphangiography (MRL) of the legs. 2022;8.

17. Kikinis R, Pieper S, Vosburgh K. 3D Slicer: a platform for subject-specific image analysis, visualization, and clinical support. In: Intraoperative imaging and image-guided therapy. 2013. p. 277–289.

18. 3D Slicer [Internet]. [cited 2023 Sep 1]. Available from: https://www.slicer.org/

19. The Vascular Modeling Toolkit (VMTK) [Internet]. [cited 2023 Oct 4]. Available from: https://www.vmtk.org/

20. Mazzei MA, Gentili F, Mazzei FG, Gennaro P, Guerrieri D, Nigri A, et al. High-resolution MR lymphangiography for planning lymphaticovenous anastomosis treatment: a single-centre experience. Radiologia Medica [Internet]. 2017 Dec 2 [cited 2019 Oct 7];122(12):918–27. Available from: http://link.springer.com/10.1007/s11547-017-0795-x

21. Liu NF, Yan ZX, Wu XF, Luo Y. Magnetic resonance lymphography demonstrates spontaneous lymphatic disruption and regeneration in obstructive lymphedema. Lymphology. 2013;46(2):56–63.

22. Zhou G xing X, Chen X, Zhang J hua H, Zhu J qi Q, Wang Y bin Bin, Wang Z qiu Q. MR lymphangiography at 3.0 Tesla to assess the function of inguinal lymph node in low extremity lymphedema. Journal of Magnetic Resonance Imaging [Internet]. 2014 Dec 1 [cited 2019 Oct 7];40(6):1430–6. Available from: http://doi.wiley.com/10.1002/jmri.24499

23. Borri M, Schmidt MA, Gordon KD, Wallace TA, Hughes JC, Scurr ED, et al. Quantitative Contrast-Enhanced Magnetic Resonance Lymphangiography of the Upper Limbs in Breast Cancer Related Lymphedema: An Exploratory Study. Lymphat Res Biol. 2015 Jun 1;13(2):100–6.

24. Soga S, Onishi F, Jinzaki M, Mikoshi A, Minabe T, Shinmoto H. Analysis of collateral lymphatic circulation in patients with lower limb lymphedema using magnetic resonance lymphangiography. J Vasc Surg Venous Lymphat Disord. 2021;9(2):471--481.e1.

25. Yamamoto T, Narushima M, Doi K, Oshima A, Ogata F, Mihara M, et al. Characteristic indocyanine green lymphography findings in lower extremity lymphedema: The generation of a novel lymphedema severity staging system using dermal backflow patterns. Plast Reconstr Surg. 2011;127(5):1979–86.

26. Sarica M, Gordon K, Van Zanten M, Heenan S, Mortimer P, Irwin A, et al. Lymphoscintigraphic abnormalities associated with Milroy disease and Lymphedema-Distichiasis syndrome. Lymphat Res Biol. 2019;17(6):610–9.

27. Crescenzi R, Donahue PMC, Hartley KG, Desai AA, Scott AO, Braxton V, et al. Lymphedema evaluation using noninvasive 3T MR lymphangiography. Journal of Magnetic Resonance Imaging. 2017 Nov 1;46(5):1349–60.

28. Mills M, Brezgyte G, Ho B, Pearce J, Gordon K, Mortimer PS, et al. DCE-MR Lymphangiography Demonstrates Significantly Different Lymphatic Drainage in Patients with a FOXC2 Gene Mutation Compared to Controls. In: Proceedings of the 31st ISMRM Annual Meeting Annual Meeting of the International Society for Magnetic Resonance in Medicine (ISMRM). 2023.

29. Arrivé L, Derhy S, Dahan B, El Mouhadi S, Monnier-Cholley L, Menu Y, et al. Primary lower limb lymphoedema: classification with non-contrast MR lymphography. Eur Radiol. 2018 Jan 1;28(1):291–300.

30. Kim G, Smith MP, Donohoe KJ, Johnson AR, Singhal D, Tsai LL. MRI staging of upper extremity secondary lymphedema: correlation with clinical measurements. Eur Radiol. 2020;30(8):4686–94.

31. Gennaro P, Borghini A, Chisci G, Mazzei FG, Weber E, Tedone Clemente E, et al. Could MRI visualize the invisible? An Italian single center study comparing magnetic resonance lymphography (MRL), super microsurgery and histology in the identification of lymphatic vessels. Eur Rev Med Pharmacol Sci. 2017;21(4):687–94.

32. Maki JH, Neligan PC, Briller N, Mitsumori LM, Wilson GJ. Dark Blood Magnetic Resonance Lymphangiography Using Dual-Agent Relaxivity Contrast (DARC-MRL): A Novel Method Combining Gadolinium and Iron Contrast Agents. Curr Probl Diagn Radiol. 2016 May;45(3):174–9.

33. Sibley RC, Moroz MA, Vasanawala SS, Loening AM. Iron Oxide Nanoparticle Magnetic Resonance Lymphangiography (ION-MRL): A New Technique for Imaging the Peripheral and Central Lymphatic System. In: Proceedings of the 30th ISMRM Annual Meeting Annual Meeting of the International Society for Magnetic Resonance in Medicine (ISMRM). 2022.

34. Cellina M, Oliva G, Menozzi A, Soresina M, Martinenghi C, Gibelli D. Non-contrast Magnetic Resonance Lymphangiography: an emerging technique for the study of lymphedema. Clin Imaging. 2019 Jan 1;53(September 2018):126–33.

35. Lohrmann C, Foeldi E, Langer M. Indirect magnetic resonance lymphangiography in patients with lymphedema preliminary results in humans. Eur J Radiol. 2006 Sep;59(3):401–6.

36. Lohrmann C, Foeldi E, Speck O, Langer M. High-resolution MR lymphangiography in patients with primary and secondary lymphedema. American Journal of Roentgenology. 2006;187(2):556–61.

37. Kashyap V, Gharleghi R, Li DD, McGrath-Cadell L, Graham RM, Ellis C, et al. Accuracy of vascular tortuosity measures using computational modelling. Sci Rep. 2022;12(1):1–10.

38. Crescenzi R, Donahue PMC, Garza M, Lee CA, Patel NJ, Gonzalez V, et al. Elevated magnetic resonance imaging measures of adipose tissue deposition in women with breast cancer treatment-related lymphedema. Breast Cancer Res Treat. 2022;191(1):115–24.

39. Shinaoka A, Kamiyama K, Yamada K, Kimata Y. A new severity classification of lower limb secondary lymphedema based on lymphatic pathway defects in an indocyanine green fluorescent lymphography study. Sci Rep. 2022;12(1):1–11.

40. Mansour S, Josephs KS, Ostergaard P, Gordon K, Van Zanten M, Pearce J, et al. Redefining WILD syndrome: a primary lymphatic dysplasia with congenital multisegmental

lymphoedema, cutaneous lymphovascular malformation, CD4 lymphopaenia and warts. J Med Genet. 2023 Jan 1;60(1):84–90.

Table 1. Study participant characteristics.

Characteristic	
Overall	
Age (years)	37.6 ± 11.2 (range = 23.5 – 69.0)
Sex, n (%)	
Male	10 (40.0)
Female	15 (60.0)
Limbs Excluded	1
Injection protocol optimisation	
Contrast volume / injection (mL)	*# of limbs analysed (F/M)*
0.45	7/3
0.1	4/2
0.02	1/1
Main study	
Contrast volume / injection (mL)	*# of limbs analysed (F/M)*
0.45	18/13

Table 2 MR protocol details.

	Anatomy	Orientation	TR / TE (ms)	FA (^{0})	Voxel Size (mm)		NSA	Fat Suppression	SENSE Factor (Direction)
					Acquired	Reconstructed			
T_2 weighted TSE	Leg	Coronal	2800 / 565	90	2.0 x 2.0 x 3.0	1.2 x 1.2 x 1.5	2	SPAIR	1.6 (RL) 1.6 (AP)
T_1 weighted SPGR	Leg	Coronal	3.7 / 1.6	12	1.0 x 1.0 x 1.0	0.6 x 0.6 x 0.8	1	SPAIR	1.6 (RL) 1.6 (AP)
T_1 Dixon	Thigh	Coronal	4.4 / 1.4, 2.6	10	1.0 x 1.0 x 1.0	0.7 x 0.7 x 0.8	1	N/A	1.6 (RL) 1.6 (AP)

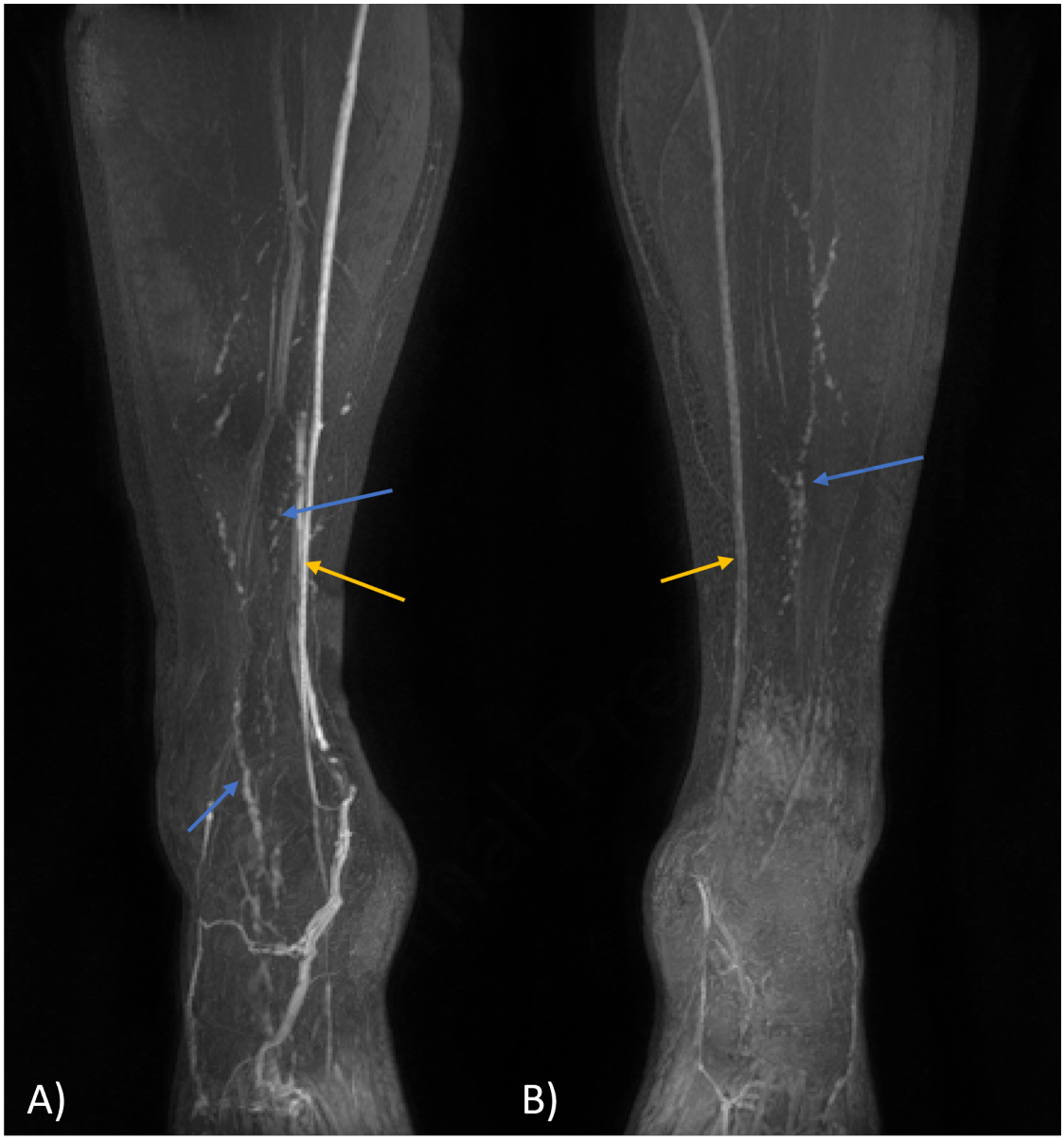
A)
B)


A)
B)

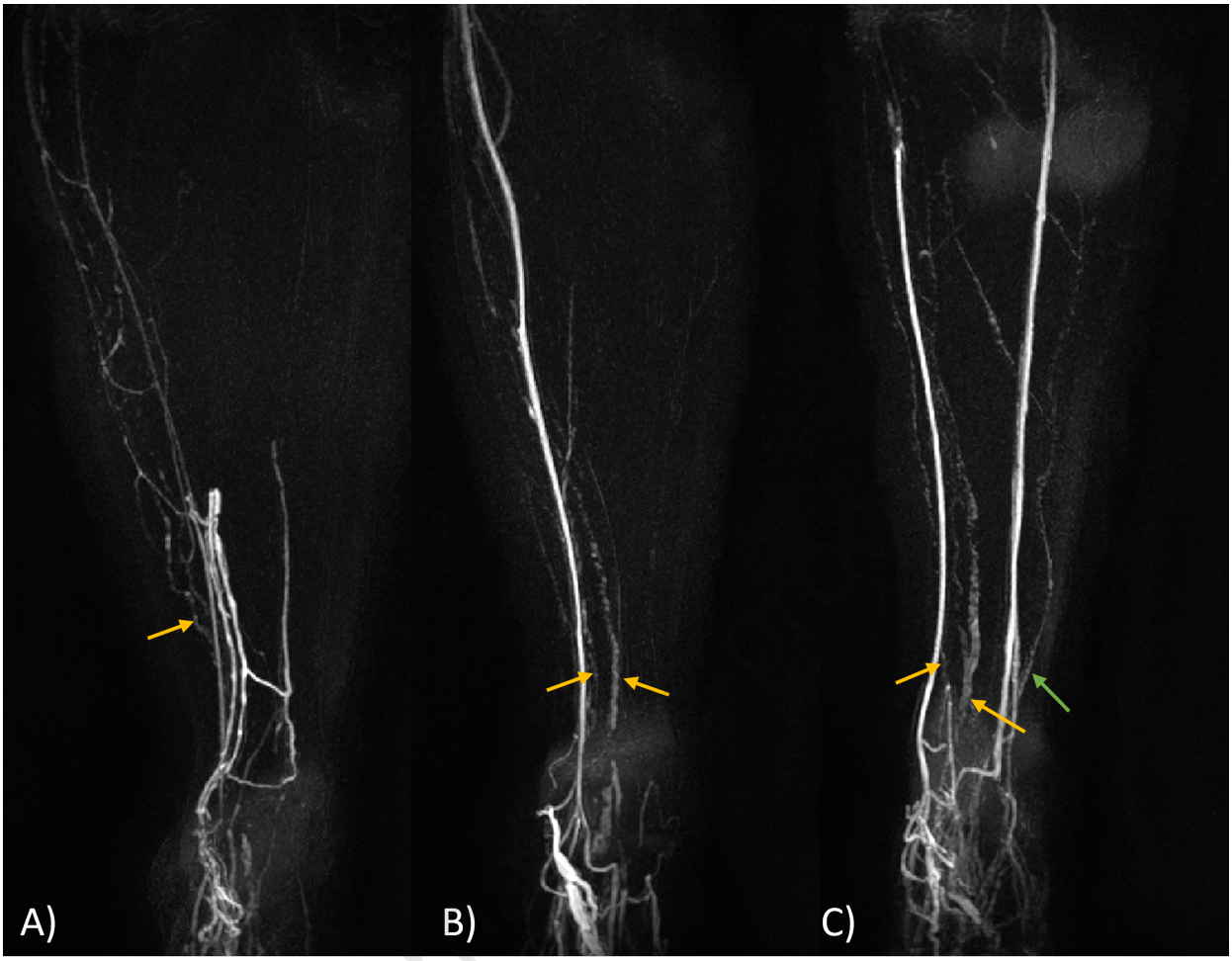

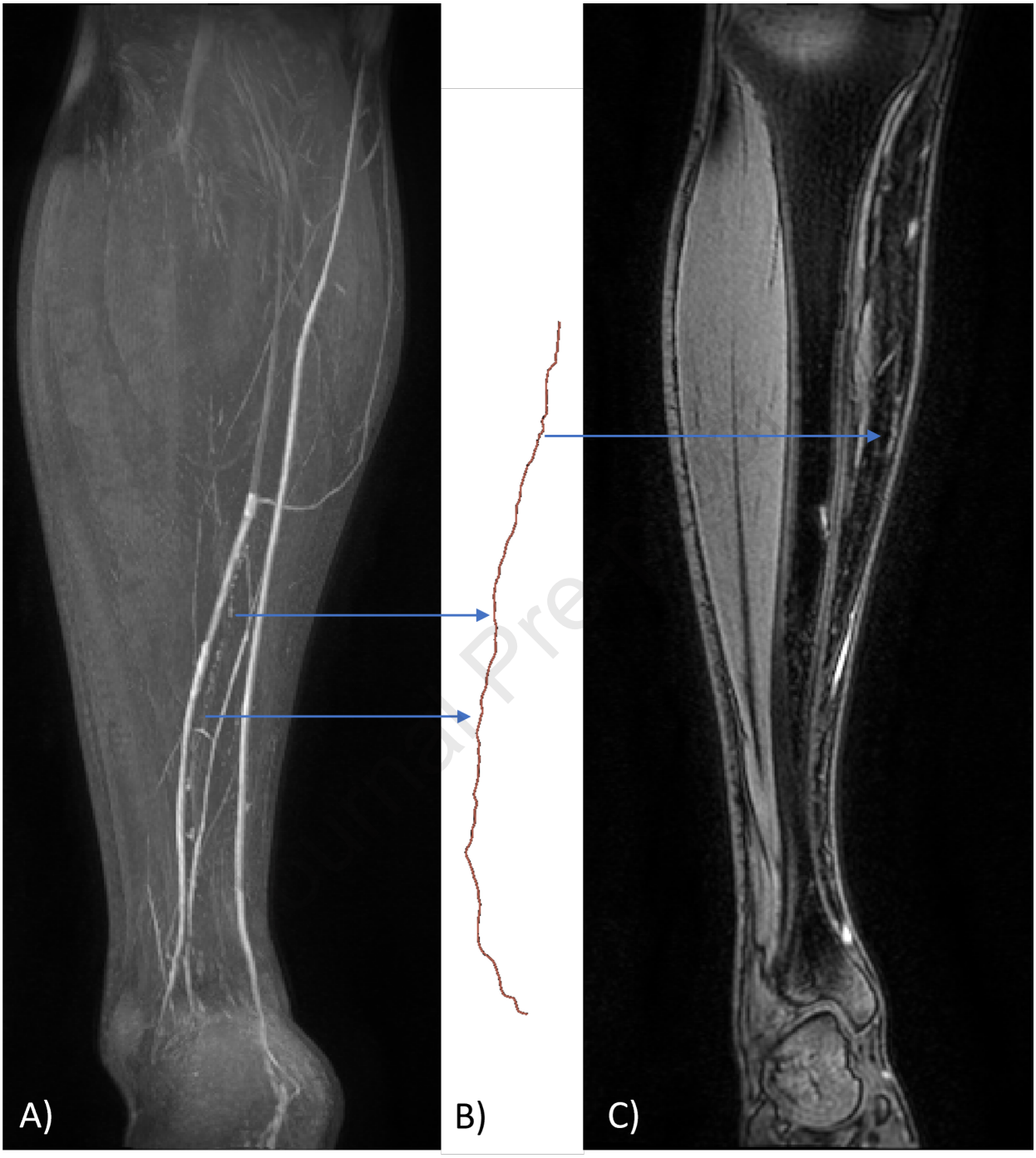
A)
B)
C)

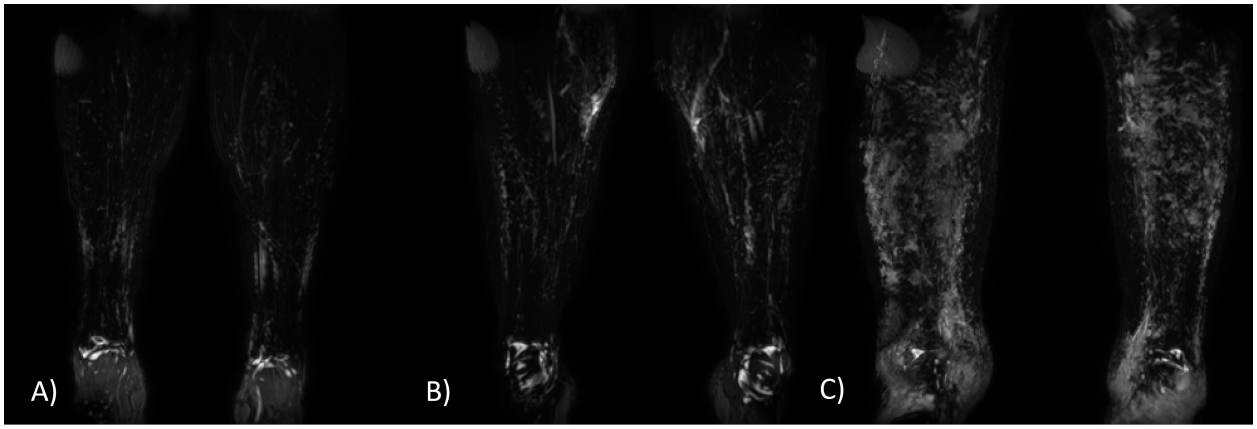

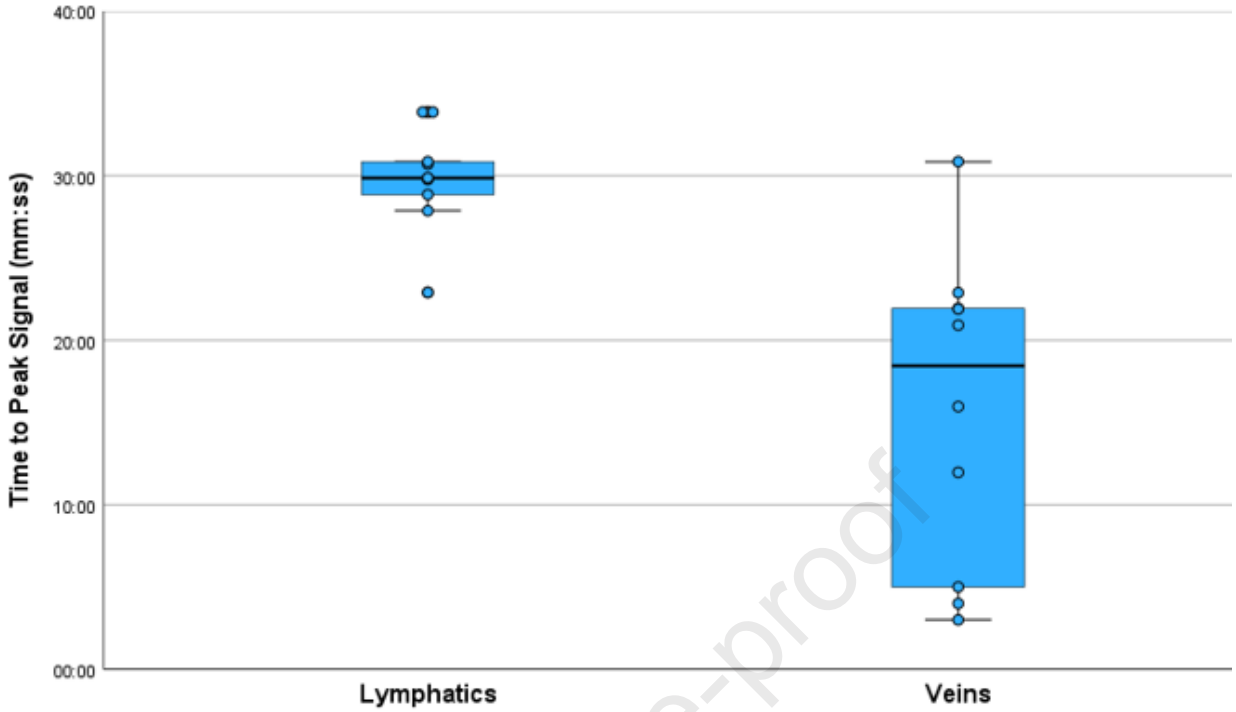

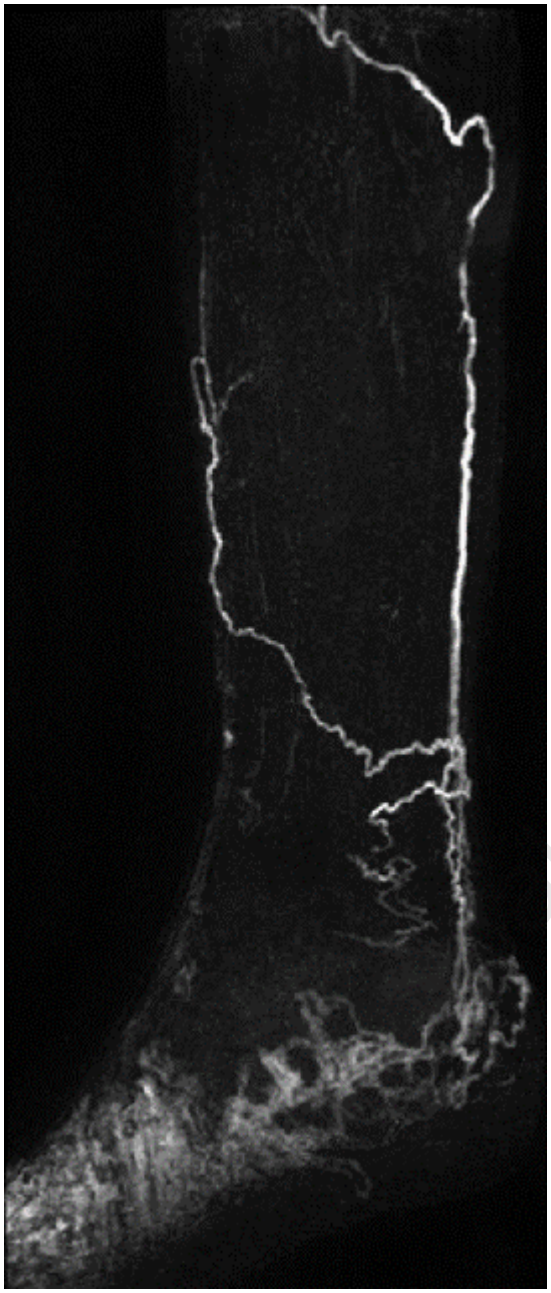

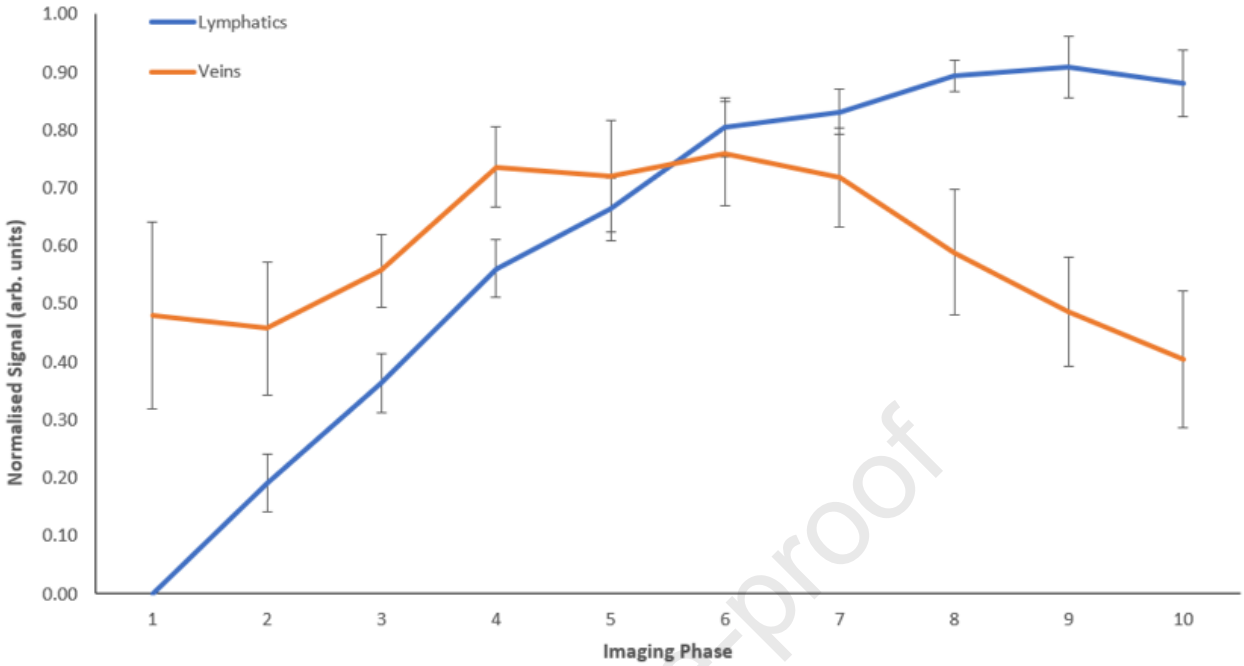

Table 1: Study participant characteristics.

Table 2: Magnetic Resonance Imaging protocol details.

Figure 1: Injection protocol optimisation detects differences in lymphatic vessel visibility. Bilateral coronal maximum intensity projection (MIP) images acquired in a 23-year-old female. 4 x 1ml inter-digital contrast injections were administered into the dermis of each foot. The right leg (A) was injected with a Gadolinium-based contrast agent (GBCA) at a concentration of 0.45mL GBCA / mL and the left (B) with 0.1mL GBCA / mL. In the limb receiving a higher GBCA concentration, both veins (orange arrows) and lymphatic (blue arrows) vessels appear brighter. Images are displayed with the same window and level and at approximately the same timepoint post-contrast injection.

Figure 2: Lymphatic vessel anatomy and function can be visualised. Left leg of a 25-year-old female showing lymphatic (blue arrows) and venous (orange arrow) vessels approximately 20 minutes after T_1 weighted spoilt gradient echo imaging commenced following contrast administration. A maximum intensity projection (MIP) is shown in frame (A) following subtraction of the first post-contrast image, while in (B) we see a single coronal image slice of the same timepoint with the approximate location at which lymphatic signal was assessed shown with an orange hashed box (enlarged for better visibility).

Figure 3: Examples demonstrating a range of vessel numbers and both anteromedial and anterolateral pathways. Coronal subtraction maximum intensity projections for the left leg of three female participants showing 1 (A), 2 (B), and 3 (C) lymphatic vessels observed at the level of the ankle approximately 20 minutes after T_1 weighted post-contrast imaging commenced. The leg shown in frame (C) also demonstrates clear anterolateral lymphatic drainage highlighted by the green arrow, while anteromedial vessels are shown with the orange arrows. All limbs also show clear venous enhancement. Note that the locations of the arrows do not correspond to the location at which lymphatic diameter was estimated.

Figure 4: Vessel segment analysed for tortuosity. Post-contrast images of the left leg of a 31-year-old male. Frames (A) and (C) show MIP and single slices respectively demonstrating the lymphatic vessel which was segmented and displayed in (B), and whose tortuosity was measured at 1.04. Note how the lymphatic becomes obscured by overlying blood vessels in (A) but can still be clearly observed in the individual coronal slice (C). Supplementary videos 1 and 2 display vessel segment and subtraction MIP for this limb rotational 3D projections.

Figure 5: Examples demonstrating a range of T_2 weighted images from controls and lymphoedema patients. Single slices heavily T_2 weighted images mid-leg for 31- (A), 37- (B) and 27- (C) year-old women. The 37-year-old healthy control participant showed the most extensive hypointense regions on their T_2 weighted images (B) of any control included in this study. For comparison, frame (C) demonstrated a T_2 weighted scan from a similarly aged lymphoedema patient (diagnosed with WILD syndrome [40]), with extensive high signal, fluid rich, regions throughout the entire limb. Based purely on a physical inspection of the limbs, the clinician performing contrast injection suggested that an undiagnosed lipoedema could be present for the individual shown in (B) which may explain the increased fluid signal. (A)-(C) are shown with identical image windowing and were obtained using the same imaging protocol.

Figure 6: Time to peak signal in lymphatic and venous vessels. Boxplot displaying the time elapsed between the start of contrast injection in a limb and the time at which peak signal was measured in either an anteromedial lymphatic vessel (e.g. the region shown in Figure 2) or the long saphenous vein just superior to the ankle. In the 10 vessels assessed, the lymphatic signal peaked on average

significantly later than the venous signal (15:50 ± 03:06 vs. 29:50 ± 09:29 mm:ss; mean ± standard deviation). Note that for 4/10 of the lymphatic vessels the peak signal was observed in the final imaging phase.

Figure 7: Abnormal tortuous lymphatics in a lymphoedema patient. Sagittal T_1 weighted subtraction MIP for a 48-year-old male with a genetically confirmed Milroy diagnosis, demonstrating abnormal appearing lymphatic vessels and lymphatic vessels traversing the posterior of the limb. Image obtained using inter-digital contrast injection and moderately T_1 weighted 3D spoilt gradient echo imaging, as described in this study.

Supplementary Figure 1: Normalised average uptake curves in the lymphatics and long saphenous vein showing the gradual increase in lymphatic signal across the 10 post-contrast imaging phases (approx., 30 minutes) compared to a more rapid wash-in and wash-out seen in the veins. For each vessel the signal was transformed to take a value between 0-1 before averaging across the 10 vessels. Error bars = standard error of the mean.

Supplementary Video 1: Post-contrast rotational maximum intensity projections of the left leg of a 31-year-old male demonstrating anteromedial lymphatic vessels (see also Figure 4).

Supplementary Video 2: Video demonstrating a segmented anteromedial lymphatic vessel of the left leg of a 31-year-old male also shown in Figure 4 and Supplementary Video 1. Lymphatic vessels were segmented in 10 limbs to estimate tortuosity (the ratio of their length to the distance between their end points). Segmentations, and this video, were created using the open-source 3D Slicer software (version 5.2.2).

Supplementary Table 1. Lymphatic vessel pathways and number observed crossing the anterior ankle for the 16 participants imaged following contrast optimisation.

Participant #	Age (years)	# of Vessels Crossing Ankle		Pathways Present			
				Anteromedial		Anterolateral	
		L	R	L	R	L	R
1	29.1	3	3	X	X		X
2	69.0	3	1		X	X	
3	41.1	2	3	X	X		X
4	25.9	1	1	X	X		
5	53.4	3	N/A	X	N/A		N/A
6	31.7	3	1	X	X		
7	37.3	1	2	X	X		
8	47.0	1	2	X	X		
9	36.5	2	2	X	X		
10	37.5	1	3	X	X		
11	55.4	3	2	X	X		
12	42.1	0	2		X		
13	40.7	3	3	X	X	X	
14	33.2	2	4	X	X		X
15	25.8	2	2	X	X		
16	51.2	3	3	X	X		X

Note that during imaging the right leg of participant 5 suffered severe signal loss and could not be analysed.